Journal of Power Sources 253 (2014) 419–423

Contents lists available at ScienceDirect

Journal of Power Sources

journal homepage: www.elsevier.com/locate/jpowsour

Short communication

Performance of Al–0.5 Mg–0.02 Ga–0.1 Sn–0.5 Mn as anode for Al–air battery in NaCl solutions

Jingling Ma [a,b], Jiuba Wen [a,*], Junwei Gao [a], Quanan Li [a]

[a] School of Materials Science and Engineering, Henan University of Science and Technology, Luoyang 471003, PR China
[b] Collaborative Innovation Center of Nonferrous Metals, Henan Province, Henan University of Science and Technology, Luoyang 471003, PR China

HIGHLIGHTS

- Al–air battery based on Al–Mg–Ga–Sn–Mn offers higher electrochemical performance.
- The corrosion potential of Al–Mg–Ga–Sn–Mn is −1.499 V (SCE).
- At 20 mA cm^{-2}, the operating voltage of Al–air battery with Al–Mg–Ga–Sn–Mn is 1.236 V.
- The anodic utilization of Al–air battery with Al–Mg–Ga–Sn–Mn is 85.3%.

ARTICLE INFO

Article history:
Received 15 September 2013
Received in revised form
7 December 2013
Accepted 12 December 2013
Available online 20 December 2013

Keywords:
Aluminum alloy
Air battery
Potential
Self-corrosion

ABSTRACT

In this research, metal–air battery based on Al, Zn, Al–0.5 Mg–0.02 Ga–0.1 Sn and Al–0.5 Mg–0.02 Ga–0.1 Sn–0.5 Mn (wt%) is prepared and the battery performance is investigated by constant current discharge test in 2 mol L^{-1} NaCl solutions. The characteristics of the anodes after discharge are investigated by electrochemical impedance spectroscopy (EIS), scanning electron microscopy (SEM). The corrosion behavior of the anodes is studied by self-corrosion rate measurement and potentiodynamic polarization measurement. The results show that Al–Mg–Ga–Sn–Mn is more active than Al, Zn and Al–Mg–Ga–Sn anodes. The self-corrosion rate is found to be in the order: Al < Al–Mg–Ga–Sn–Mn < Al–Mg–Ga–Sn < Zn. It has been observed that the Al–air battery based on Al–Mg–Ga–Sn–Mn offers higher operating voltage and anodic utilization than those with others. SEM and EIS results of the alloy are in good agreement with corrosion characteristics.

1. Introduction

Owing to the low atomic mass of aluminum, high energetic capacity (2980 Ah kg^{-1}), along with the negative value of standard electrode potential (−1.66 V vs. Normal Hydrogen Electrode), low cost, and no pollution, Al–air battery is a promising power source and energy storage device [1–3]. However currently, the Al–air battery is still not as popular as Zn–air battery [4]. The major problem is that Al anode exhibited some less attractive properties, such as the severe self-corrosion during battery discharge [5,6], and these disadvantages have delayed the development of Al–air battery and limited its commercial exploitation. Due to presence of oxide film, the corrosion potential of Al anode is shifted in the positive direction (about −0.8 V vs. NHE), and the active dissolution of Al is slowed down considerably [7,8].

One way to enhance the Al anode performance is to alloy Al with other elements. The addition of alloying elements such as Mg, Ga, Hg, and Sn can shift the potential towards more negative, causing the so-called activation of Al [9–11]. This wasteful self-corrosion results in severe capacity loss and low anodic efficiency. For the purpose of reducing the self-corrosion of Al anode the measures were taken: use alloying with the elements of high hydrogen overpotential such as Pb, Zn and Sn, etc [12–14]. The paper investigated the microstructure and electrochemical performance of Al–Mg–Ga–Sn alloy [15]. In order to further reduce the self-corrosion of the alloy, it is necessary reducing the harmful effects of impurity Fe element. Mn element can be come into being Al_6 (Mn, Fe) in the alloy and the potential of Al_6 (Mn, Fe) is almost the same with that Al based, thereby reducing the harmful effects of the impurities Fe [16,17].

The effect of Mn elements on the microstructure and electrochemical performance of Al anode alloys in sodium chloride solution was studied in our preliminary research. The electrochemical behavior of Al–0.5 Mg–0.02 Ga–0.1 Sn–0.5 Mn alloy as anode of Al–air battery was studied in this paper. The commonly electrolyte

* Corresponding author. Tel.: +86 379 64231846; fax: +86 379 64230597.
E-mail address: wenjiuba52@126.com (J. Wen).

0378-7753/$ – see front matter © 2013 Elsevier B.V. All rights reserved.
http://dx.doi.org/10.1016/j.jpowsour.2013.12.053

used in Al–air battery was alkaline solution or neutral NaCl solutions [18,19]. The high self-corrosion rate of aluminum in the concentrated alkaline solutions is known [20]. The present work is aimed to study the corrosion behavior of Al–Mg–Ga–Sn–Mn anode in 2 mol L^{-1} NaCl solutions. The electrochemical behavior of Al, Zn and Al–0.5 Mg–0.02 Ga–0.1 Sn anodes as contrast material will be considered.

2. Experimental

2.1. Material preparation

Raw materials are commercial pure aluminum, zinc, magnesium ingots, gallium particle, tin particle (>99.9%), Al–10% wt Mn master alloy for casting the experiment alloys. The nominal composition of the experiment alloys are 0.5% wt Mg–0.02% wt Ga–0.1% wt Sn–Al, 0.5% wt Mg–0.02% wt Ga–0.1% wt Sn–0.5% Mn–Al. Raw material ingots were cut, dried, weighed the required amount of materials and melted in a corundum crucible in ZGJL0.01–4C-4 vacuum induction furnace under argon atmosphere at 760 ± 5 °C. The molten alloy was poured in a preheated cast iron dye.

2.2. Electrochemical measurements

The electrochemical tests were carried out with three electrodes system at room temperature (25 ± 2 °C) by CHI660C electrochemical test system (CHI Company, USA). A saturated calomel electrode (SCE) served as the reference electrode and a Pt sheet was used as the counter electrode. The working electrodes of open circuit potential (OCP) measured with an exposed area of 1 cm^2. The samples were ground with emery paper (grade 400–800–1000–2000) and then cleaned with triply distilled water. Measurements were performed in 2 mol L^{-1} NaCl solutions for 1 h. The potentiodynamic cyclic polarization was measured at a scan rate of 1 mV s^{-1} after OCP measurement. The EIS measurements were carried out at open circuit potential with a 5 mV sine perturbation in 2 mol L^{-1} NaCl solutions. The measuring frequency range was 100 kHz–0.1 Hz.

2.3. Self-corrosion

The samples of self-corrosion tests were cut to Φ11.4 mm × 5 mm, then ground with emery paper (grade 400–800–1000–2000) and immersed in 2 mol L^{-1} NaCl solutions for 48 h. The weight of the samples before and after immersion was measured after cleaning the corrosion products formed on the sample surface. The corrosion products were clean-out in solutions of 2% CrO_3 and 5% H_3PO_4 at 80 °C for about 5 min, then rinsed by distilled water and ethanol.

The corrosion rate was calculated using the formula:

$$\text{Corrosion rate} = \text{Weight loss/surface area/time of immersion}\ (\text{mg cm}^{-2}\ \text{h}^{-1}).$$

2.4. Battery test

The batteries consisted of anode, cathode and electrolyte, where anodes were Al, Zn, Al–0.5 Mg–0.02 Ga–0.1 Sn and Al–0.5 Mg–0.02 Ga–0.1 Sn–0.5 Mn, cathode was air electrode with MnO_2 catalyst, and electrolyte was neutral 2 mol L^{-1} NaCl solution. The discharge performance of metal–air batteries was studied by means of constant current discharge test, constant current discharge test was determined at current densities of 20 mA cm^{-2} for a duration of 5 h. The discharge performance is tested using the LAND test system. The weight of anode consumed was determined from the weight of the anodes before and after discharge. The samples surface after discharge was examined using JSM-5610LV scanning electron microscope.

The anode utilization was calculated using the formula:

$$\text{Anode utilization } \eta = I_{\text{polarization}}\, h/(mF/9.0).$$

where η is the anode utilization, %; $I_{\text{polarization}}$ the polarization current of anode, A; m the weight loss, g; F the faraday constant, h the time, s.

The above electrochemical parameter values are the average of the repeated test for more than three times.

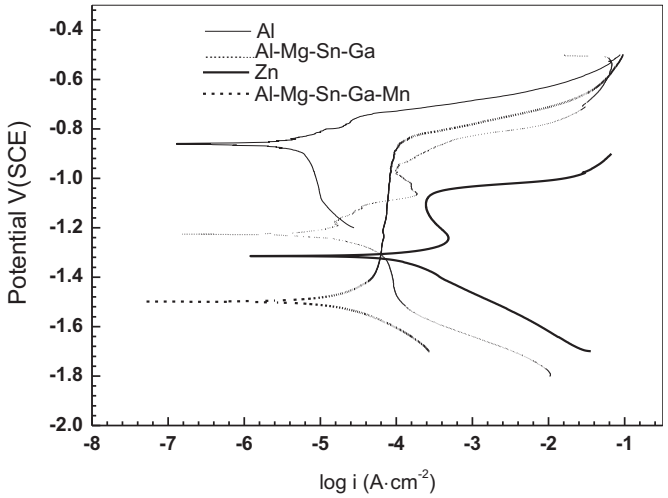

Fig. 1. Potentiodynamic polarization curves for Al, Zn, Al–Mg–Ga–Sn and Al–Mg–Ga–Sn–Mn measured in 2 mol L^{-1} NaCl solutions at a scan rate of 1 mV s^{-1}.

3. Results and discussion

3.1. Potentiodynamic polarization

Fig. 1 and Table 1 presents the potentiodynamic polarization curves and corresponding corrosion parameters of Al, Zn, Al–Mg–Ga–Sn and Al–Mg–Ga–Sn–Mn measured in 2 mol L^{-1} NaCl solutions, respectively. The corrosion potential of Al–Mg–Ga–Sn–Mn (−1.499 V) is more negative than that of Zn (−1.317 V), Al–Mg–Ga–Sn (−1.226 V) and Al (−0.862 V), which means that Al–Mg–Ga–Sn–Mn has higher electrochemical activity. The electrochemical activity increases in the following order: Al < Al–Mg–Ga–Sn < Zn < Al–Mg–Ga–Sn–Mn. The corrosion current density (I_{corr}) of Zn is much greater than that of Al, Al–Mg–Ga–Sn and Al–Mg–Ga–Sn–Mn, implying that Zn is less corrosion resistant and the biggest self-corrosion rate than that of the others.

Table 2 shows the self-corrosion rate of the four materials, which is obtained by weight loss measurement in 2 mol L^{-1} NaCl solutions for 48 h. As illustrated in Table 2, the self-corrosion rate increases in the following order: Al < Al–Mg–Ga–Sn–Mn < Al–

Table 1
Corrosion parameters of different materials in 2 mol L^{-1} NaCl solutions.

Material	E_{corr} (V vs. SCE)	I_{corr} (A cm^{-2})	R_p (Ω cm^2)
Al	−0.862	1.072×10^{-5}	4742
Zn	−1.317	3.654×10^{-4}	152
Al–Mg–Ga–Sn	−1.226	3.795×10^{-5}	1433
Al–Mg–Ga–Sn–Mn	−1.499	2.93×10^{-5}	1475

Table 2
Corrosion rates of different materials in 2 mol L^{-1} NaCl solutions.

Material	Weight loss/mg	Corrosion rate/mg cm^{-2} h^{-1}	Corrosion rate/cm $year^{-1}$
Al	0.57	0.0013	0.0004
Zn	30.91	0.1994	0.0245
Al–Mg–Ga–Sn	10.36	0.0475	0.0154
Al–Mg–Ga–Sn–Mn	6.56	0.0301	0.0098

Mg–Ga–Sn < Zn. Al–Mg–Ga–Sn–Mn shows much lower self-corrosion rate than Zn and Al–Mg–Ga–Sn. The more positive potential and the less self-corrosion rate of Al result from the presence of compact oxide film on Al surface according to the reaction (1). The higher self-corrosion rate of Zn results from the not very compact oxide film on Zn surface according to the following reaction (2).

$$2Al + 6H_2O \rightarrow 2Al(OH)_3\downarrow + 3H_2 \quad (1)$$

$$Zn + 2H_2O \rightarrow Zn(OH)_2 + H_2 \quad (2)$$

Al alloying with Mg, Ga, Sn and Mn, namely Al–Mg–Ga–Sn–Mn anode possesses the more negative potential and the less self-corrosion rate. Based on the above analysis, in contrast to Al and Al–Mg–Ga–Sn, Al–Mg–Ga–Sn–Mn could be used in Al–air battery as anode.

3.2. Battery performance

Fig. 2 shows the discharge behavior of metal–air battery with different anodes at current densities of 20 mA cm^{-2}. The voltage–time curves are similar for all the samples. The operating voltage decreased rapidly in the early discharging stage, which is caused by the battery internal resistance, and then reached to an approximate constant value. It should be noted that the operating voltage of air battery with Al–Mg–Ga–Sn–Mn is higher than those of the others.

Table 3 summarizes the performance of the above batteries at 20 mA cm^{-2}. As shown in Table 3, the battery with Al–Mg–Ga–Sn–Mn displays higher operating voltage and anodic utilization than those of the others. The anodic utilization of Al is higher than that of Zn and Al–Mg–Ga–Sn; this is because the low self-corrosion rate of Al resulted from the formation of the protective oxide film on Al surface. Among all the samples, the best performance of battery with Al–Mg–Ga–Sn–Mn is obtained, the

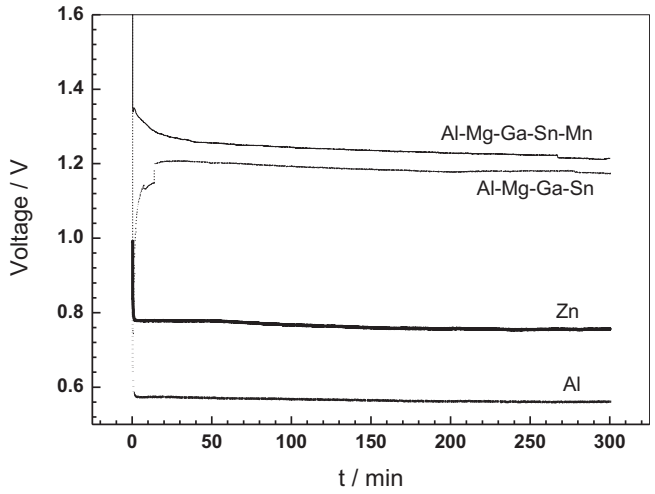

Fig. 2. Discharge behavior of metal–air battery with different anodes.

Table 3
The discharge performance of metal–air battery with different anodes.

Material	Operating voltage (V)	Anodic efficiency (%)
Al	0.565	81.4
Zn	0.759	68.1
Al–Mg–Ga–Sn	1.185	63.2
Al–Mg–Ga–Sn–Mn	1.236	85.3

operating voltage is 1.236 V and the anodic utilization is 85.3%. Improved discharge characteristics may be due to the Mn element of the alloy reducing the harmful effects of impurity Fe element, which results in a decrease of self-corrosion [21,22].

3.3. Surface analysis after discharge

The surface morphologies of different anodes after discharge at 20 mA cm^{-2} current densities for 5 h in 2 mol L^{-1} NaCl solution were obtained by scanning electron microscopy examination. The results are shown in Fig. 3, it could be seen that the morphology of Al shows few small pits in Fig. 3a. As can be observed in Fig. 3c and d, the morphologies of Al–Mg–Ga–Sn and Al–Mg–Ga–Sn–Mn anodes after discharge, are loose with many pores and cracks compare with Fig. 3a and b. The relative passivity morphology of Al results from the surface hydroxide layer according to the following reaction.

$$4Al + 3O_2 + 6H_2O \rightarrow 4Al(OH)_3 \quad (3)$$

Pure aluminum, is unsuitable for use as the anode of an Al–air battery since its surface is covered by a passive hydroxide layer creating high overpotential during anodic dissolution. Alloying aluminum with particular elements such Sn, and Ga, activates it by breaking down the passive layer. On one hand, the low melting point alloying elements Sn and Ga distribute evenly on the solid solution of Al or in the grain boundary, destroy the Al lattice, and it can't generate continuous passive film the surface; On the other hand, the alloying elements with low melting point and high hydrogen evolution overpotential dissolve and deposition on the aluminum surface again, which always make the alloy in the highly active state. The addition of Mg to aluminum improves its impurity intolerance most probably because the magnesium forms compounds with elements like silicon, preventing them from reducing on cathodic sites to act as centers for hydrogen evolution [23]. Using Mn as an alloying element has been shown to reduce the corrosion rate of aluminum which contains impurity iron. The morphology of Zn shows more intense corrosion in Fig. 3b, corrosion cover entire surface and pitting is entirely masked by uniform corrosion according to the following reaction, the corrosion product of ZnO has not a protective effect.

$$2Zn + O_2 \rightarrow 2ZnO \quad (4)$$

3.4. Electrochemical impedance spectroscopy

The EIS plots of the four anodes are shown in Fig. 4. The plots consisted of two loops. The high frequency loop might be resulted from charge transfer; the middle frequency loop might be due to the dissolution precipitation (an aggregating layer) on the alloy surface [24]. An equivalent circuit for simulating this process is shown in Fig. 5 and the fitting values of impedance parameters are listed in Table 4. To obtain more precious fitting results, the employed capacitance element (C) which shows the double-layer capacitance is replaced by constant phase element (CPE). In Fig. 5, R_s represents the solution resistance, R_t and CPE_1 are the charge-transfer resistance and double-layer capacitance of the alloy

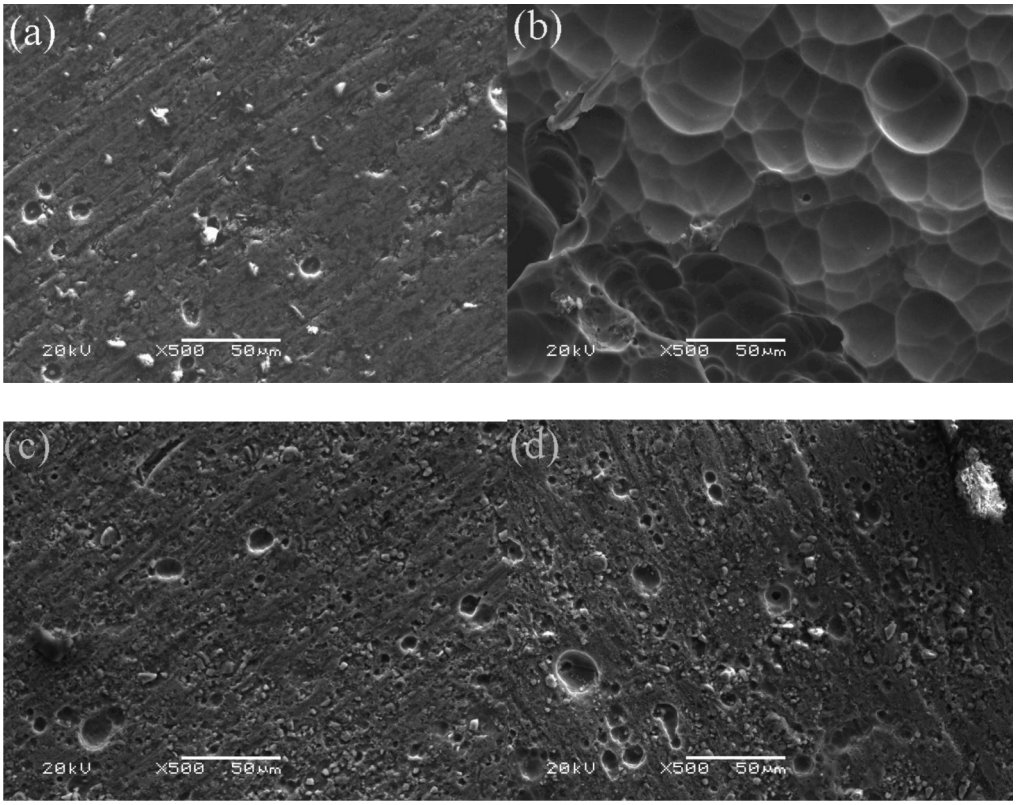

Fig. 3. SEM micrographs of anodes obtained after discharge in 2 mol L^{-1} NaCl solutions (a) Al, (b) Zn, (c) Al–Mg–Ga–Sn, and (d) Al–Mg–Ga–Sn–Mn.

surface. CPE_2 and R_2 represent corresponding parameters for the dissolution process. The fitting values obtained by ZSimpwin software for the equivalent elements are shown in Table 4. The x^2 is the precision of the simulated data. We can see that the x^2 values are small, reflecting the fact that the fitting data have good agreement with the experimental ones. In general, the higher R_t reflects a lower corrosion since the exchange current is directly associated with the electrochemical process of corrosion [25]. It can be seen that the R_t reduces in the following order: Al > Al–Mg–Ga–Sn–Mn > Al–Mg–Ga–Sn > Zn. This indicates that the corrosion process is more intense with the order. Consequently except for Al, Al–Mg–Ga–Sn–Mn could keep high anodic utilization during discharge.

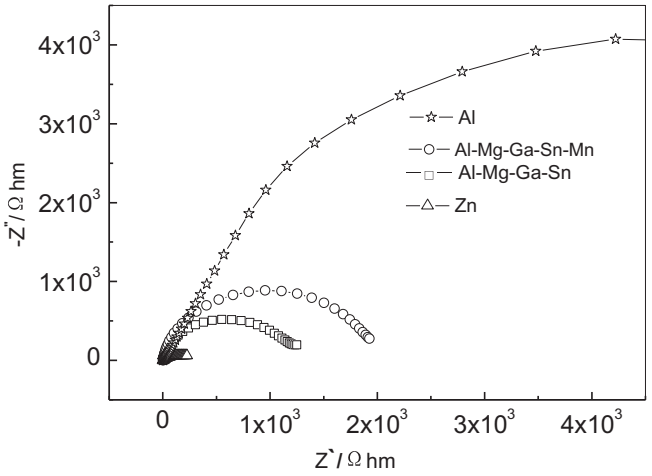

Fig. 4. EIS patterns of anodes obtained after discharge in 2 mol L^{-1} NaCl solutions.

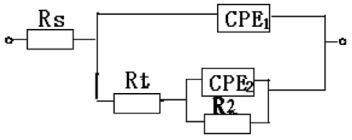

Fig. 5. Equivalent circuit of EIS of anodes obtained after discharge.

4. Conclusions

We investigated the corrosion behavior and discharge performance of Al, Zn, Al–Mg–Ga–Sn and Al–Mg–Ga–Sn–Mn anodes in 2 mol L^{-1} NaCl solutions. Compared with Zn and Al–Mg–Ga–Sn, Al–Mg–Ga–Sn–Mn has higher electrochemical performance and lower self-corrosion rate. The corrosion potential and the self-corrosion rate of Al–Mg–Ga–Sn–Mn are −1.499 V and 0.0098 cm $year^{-1}$, respectively. Using Al–Mg–Ga–Sn–Mn as anode

Table 4
EIS simulated values of anodes after discharge.

Anodes	Al	Al–Mg–Ga–Sn–Mn	Al–Mg–Ga–Sn	Zn
R_s (Ω cm^2)	2.34	3.19	3.11	2.14
CPE_1 (Ω^{-1} cm^{-2} s^{-1})	4.19×10^{-5}	7.93×10^{-5}	2.55×10^{-5}	1.85×10^{-3}
n_1 ($0 < n < 1$)	0.80	0.90	1	0.41
R_t (Ω cm^2)	9659	1234	4.53	0.035
CPE_2, (Ω^{-1} cm^{-2} s^{-1})	2.39×10^{-5}	1.19×10^{-2}	4.85×10^{-5}	1.36×10^{-4}
n_2 ($0 < n < 1$)	0.83	1	0.88	0.89
R_2 (Ω cm^2)	105	274	1975	338.1
x^2	9.16×10^{-3}	3.97×10^{-3}	1.12×10^{-3}	4.83×10^{-3}

could improve the performance of Al–air battery, and solve the problem of severe self-corrosion and passivation. At a current density of 20 mA cm^{-2}, the operate voltage of Al–air battery with Al–Mg–Ga–Sn–Mn anode is 1.236 V, and the anodic utilization is 85.3%. The morphology of Al–Mg–Ga–Sn–Mn anode after discharge was lost resulting in the high activation of the alloy. The high anodic utilization of Al–Mg–Ga–Sn–Mn anode during discharge is partially responsible for the higher R_t, which is well validated by EIS measurement.

Acknowledgment

This work was supported by Cultivation Research Innovation Ability of Henan University of Science and Technology (grant no. 2012ZCX017), Innovative Research Team (in Science and Technology) in University of Henan Province (grant no. 2012IRTSTHN008) and Science and Technique Key Program of He'nan Educational Committee (grant no. 12A430007).

References

[1] S.H.H. Yang, H. Knickle, J. Power Sources 112 (2002) 162–173.
[2] H. Wu, in: World Non-grid-connected Wind Power and Energy Conference, 2010, pp. 245–248.
[3] Z.A. Zhuk, E.A. Sheindlin, V.B. Kleymenov, I.E. Shkolnikov, Y.M. Lopatin, J. Power Sources 157 (2006) 921–926.
[4] G.M. Wu, C.C. Yang, J. Membr. Sci 280 (2006) 802–808.
[5] F. Reichel, L.P.H. Jeurgens, E.J. Mittemeijer, Acta Mater. 12 (2008) 2897–2907.
[6] Z.Q. Ma, X.X. Li, J. Solid-State Electrochem. 15 (2011) 2601–2606.
[7] S. Gudic, I. Smoljko, M. Kliškic, Electrochim. Acta 50 (2005) 5624–5632.
[8] M.A. Amin, E.R. Abd, S. Sayed, E.F. Essam, R.S. Mahmoud, N.M. Abbas, Electrochim. Acta 54 (2009) 4288–4296.
[9] S.E.A. Zein, A.Q. Saleh, J. Appl. Electrochem. 34 (2004) 331–339.
[10] W. Xiong, G.T. Qi, X.P. Guo, Z.L. Lu, Corros. Sci. 53 (2011) 1298–1303.
[11] A. Elango, V.M. Periasamy, M. Paramasivam, Anti-Corros. Meth. Mater. 56 (2009) 266–272.
[12] S.A. Mideen, M. Ganesan, M.A. Athan, K.B. Sarangapani, V. Balaramachandran, V. Kapali, S.V. Iyer, J. Power Sources 27 (1989) 235–244.
[13] I. Herraiz-Cardona, E. Ortega, V. Pérez-Herranz, Electrochim. Acta 56 (2011) 1308–1315.
[14] C.M. Quevedo, J. Genesca, in: NACE-International Corrosion Conference Series, 2008, p. 080521.
[15] M. Nestoridi, D. Pletcher, R.J.K. Wood, S.C. Wang, R.L. Jones, K.R. Stokes, I. Wilcock, J. Power Sources 178 (2008) 445–455.
[16] P. Ratchev, B. Verlinden, P. Van Houtte, Acta Metall. Mater. 43 (1995) 621–629.
[17] D.T. Alexander, A.L. Greer, Acta Mater. 50 (2002) 2571–2583.
[18] Y. Liu, G.Z. Meng, Y.F. Cheng, Electrochim. Acta 54 (2009) 4155–4163.
[19] D. Mercier, M.G. Barthés-Labrousse, Corros. Sci. 51 (2009) 339–348.
[20] R. Narayan, K.P. Sheriff, Key Eng. Mater. 20 (1987) 295–330.
[21] D.S. Gandel, N. Birbilis, M.A. Easton, M.A. Gibson, in: 18th International Corrosion Congress 2, 2011, pp. 1009–1017.
[22] J.L. Ma, J.B. Wen, J Alloys Compd. 496 (2010) 110–115.
[23] E. Ghali, Understanding, Performance and Testing, Wiley, 2010.
[24] G. Galicia, N. Pébère, B. Tribollet, V. Vivier, Corros. Sci. 51 (2009) 1789–1794.
[25] T. Hong, Y.H. Sun, W.P. Jepson, Corros. Sci. 44 (2002) 101–112.